Neuronal Dynamics and Plasticity

Network Structure And The Origin Of Synchronized Bursts In Vitro

Samora Okujeni[1,2,3*], Nila Mönig[2], Steffen Kandler[1,2,3], Oliver Weihberger[1,2,3], Ulrich Egert[1,3]

1 Bernstein Center Freiburg, University Freiburg, Freiburg, Germany
2 Neurobiology & Biophysics, Institute of Biology III, Faculty of Biology, University Freiburg, Germany
3 Biomicrotechnology, Dept. Microsystems Engineering – IMTEK, University Freiburg, Germany
* Corresponding author. E-mail address: okujeni@bcf.uni-freiburg.de

It remains an ongoing matter of research in how far different aspects in the dynamics of neuronal networks depend on particular connectivity statistics. In this study, we focus on structure and dynamics in generic networks of cortical neurons in vitro. We manipulate connectivity in these networks by pharmacological interference with morphological differentiation processes in neurons. Bringing together data from MEA recordings and from histological analyses we discuss how certain connectivity features may determine the propagation of activity and the ability of these isolated networks to self-excite themselves and to maintain recurrent activity states.

1 Introduction

Brain architectures considerably evolve driven by activity-dependent neuronal differentiation processes. The context-dependent and self-organized integration of neurons is partly reflected in the cellular morphology evolving under specific tissue-dependent constraints and input scenarios. Likewise, neurons developing in isolated cultures ex vivo integrate themselves into networks based on comparable fundamental principles. The biochemical machinery translating a specific developmental context into the adequate neuronal morphology strongly depends on proteins that regulate the dynamical properties of the cytoskeleton, i.e. structural plasticity. Control of microtubule polymerization via microtubule-associated protein 2 (MAP2) phosphorylation suggests a regulatory loop in which the Protein Kinase C (PKC) takes in a key-position [1]. Various experimental studies demonstrated that manipulation of PKC activity crucially influences neuronal differentiation processes as neurite outgrowth [2], cell migration [3] and pruning [4]. In this study, we investigate dependencies between network structure and dynamics by manipulating the PKC-dependent structural differentiation of neurons.

2 Materials and Methods

Primary cortical cell cultures were prepared as described previously [5]. Cells were derived from cortices of newborn rats by mechanical and enzymatic dissociation and plated onto polyethyleneimine-coated micro-electrode arrays (6x10 with 0.5mm and 32x32 electrodes with 0.3mm spacing; Multichannel Systems). Cultures developed in growth medium (MEM) supplemented with heat-inactivated horse serum (5%), L-glutamine (0.5mM), glucose (20mM) and gentamycin (10µg/ml) under 5% CO2 and 37°C incubator conditions. PKC inhibitor Gö6976 1µM was applied starting from DIV1. Staining against MAP2 protein was performed for morphological analysis of dendrites. Recordings were performed under culture conditions (MEA1600-BC and MEA30-1024, Multichannel Systems).

3 Results

We show that cultured cortical neurons developing under chronic inhibition of Protein Kinase C (PKC inh.) form larger dendrites due to enhanced neurite outgrowth and/or impaired pruning and further reduce cluster formation. Stronger and more compact network-wide bursts (NB) are in line with proposed higher network connectivity. Lower overall activity levels based on lower NB frequencies, however, suggest a reduced ability of network self-excitation. We hypothesize that lower activity levels and less complex bursting dynamics result from reduced inhomogeneity i.e. clustering in PKC inh. networks. Conserved isotropic propagation patterns throughout the lifetime of PKC inh. networks further point towards reduced structural reorganization and thereby preservation of the early formed homogeneous connectivity. We assess origins of NB by simultaneous recordings from up to 1000 electrodes spanning almost the entire area of developing networks of 200.000 cultured neurons. By electrical stimulation via micro-electrode arrays at different sites we further probe how activity propagates within the different network structures. We further show that homogeneous networks formed under PKC inhibition are potentially able to operate at much higher activity levels driven by electrical stimulation. We conclude that the formation of neuronal clusters in isolated networks is important for the generation of intrinsic activity by local recurrent amplification of spontaneous excitation.

References

[1] Quinlan EM, Halpain S (1996) Postsynaptic mechanisms for bidirectional control of MAP2 phosphorylation by glutamate receptors. Neuron 16:357-368.

[2] Metzger F, Kapfhammer JP (2000) Protein kinase C activity modulates dendritic differentiation of rat Purkinje cells in cerebellar slice cultures. Eur J Neurosci 12:1993-2005.

[3] Larsson C (2006) Protein kinase C and the regulation of the actin cytoskeleton. Cell Signal 18:276-284.

[4] Kano M, Hashimoto K, Chen C, Abeliovich A, Aiba A, Kurihara H, Watanabe M, Inoue Y, Tonegawa S (1995) Impaired synapse elimination during cerebellar development in PKC gamma mutant mice. Cell 83:1223-1231.

[5] Shahaf G, Marom S (2001) Learning in networks of cortical neurons. J Neurosci 21:8782-8788.

Acknowledgements

We thank Patrick Pauli and Ute Riede for technical assistance. The neuroanatomy Freiburg is gratefully acknowledged for their helpful support.

Funded by the German BMBF (FKZ 01GQ0420 & FKZ 01GQ0830) and by the EC (NEURO, No. 12788).

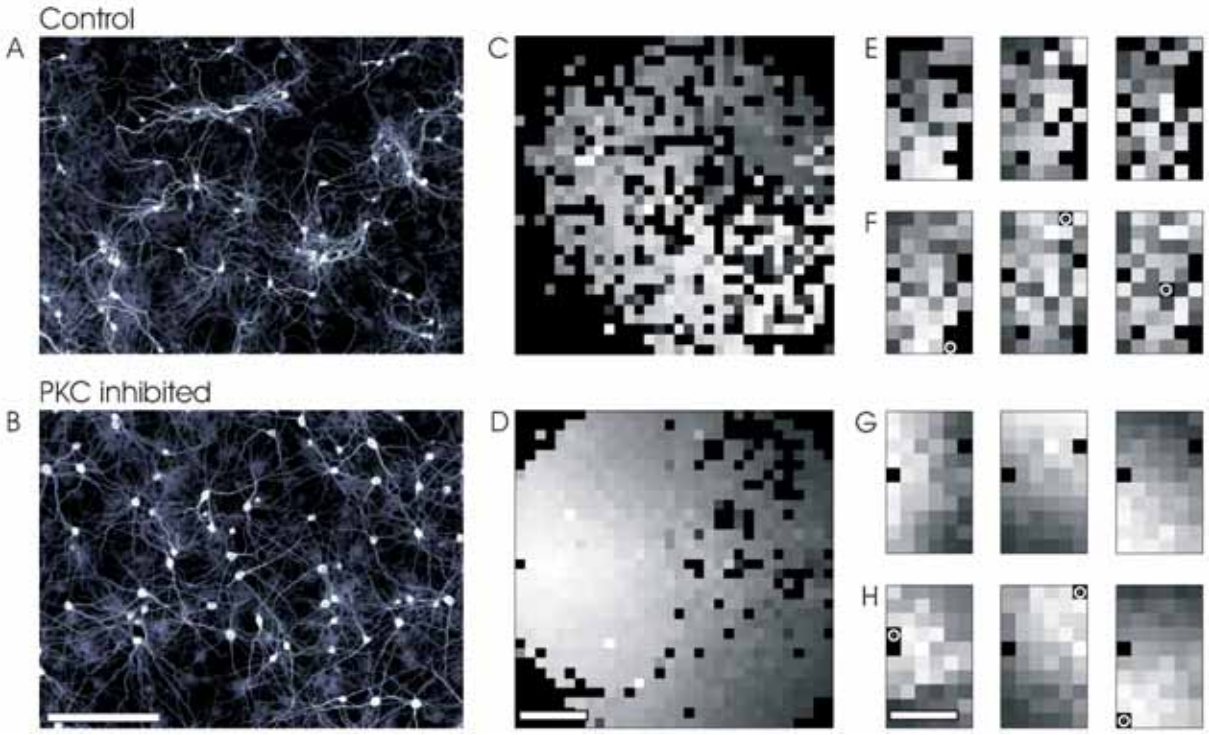

Fig. 1. Structure and dynamics in cortical cell cultures
A, B) MAP2 Staining against dendrites and somata in low density cultures (~200 neurons/mm^2) reveals reduced neuronal clustering and impaired ramification of dendrites within clusters in PKC inh. networks. Scale bars: 200µm.
C-H) Spatio-temporal propagation of activity (from early in light to late in dark gray; black indicates no activity) during network bursts onset (first spike rank order) in high density cultures (~2000 neurons/mm^2). Arrays with 1000 electrodes span almost the entire culture (C,D; corners lack neurons). PKC inh. networks show preserved isotropic propagation patterns indicating homogeneous connectivity (D). Electrical stimulation via MEAs (white circle) elicits responses with propagation patterns (H) similar to those observed in spontaneous NB (G). Networks developing under normal conditions show much more irregularity in the propagation of spontaneous (C,E) and elicited (F) activity indicating inhomogeneities in the connectivity. Scale bars: 2mm.

Software providing on-line high-resolution spatial mapping of single neurons

Patrick Dini[1,2,3*], Maxime Ambard[3], Ulrich Egert[1,3]

1 IMTEK – Department of Microsystems Engineering; University of Freiburg, Freiburg, Germany
2 Faculty of Biology; University of Freiburg, Freiburg, Germany
3 Bernstein Center for Computational Neuroscience Freiburg
* Corresponding author. E-mail address: patrick.dini@bcf.uni-freiburg.de

New tools such as High-density MEAs provide large amount of information, which help in the understanding of the geometry of single neurons and their embedding in networks activity. However, due to the complexity of such MEAs, a new software interface had to be developed, especially concerning the routing of the channels and the spike-sorting. The latter takes advantage of the capacity of the MEAs to record single neuron external electrical field potentials (EFPs) at different positions. Here we describe our strategy addressing this problem in an on-line fashion.

1 Introduction

Techniques such as patch-clamping, 2-photon microscopy and calcium imaging provide information about the electrical properties of neurons at different locations simultaneously. Nevertheless, they all suffer from trade-offs, which can be limited temporal resolution or short viability of the studied cell. To address these problems, MEAs featuring a high spatial and high temporal resolution [1] can be used. Such devices allow for the recording of the external electric field potentials emitted when a neuron fires, and thus at several locations of the neurons (see Figure 1 for an example of recorded signals). Such MEAs feature 11'016 electrodes, among which 126 are recordable simultaneously. Therefore a re-routing of the channels must be applied in order to target the subset of electrodes recording the activity of the desired neurons. Furthermore, the high spatial resolution was used here to developed an on-line spike-sorter and to compute footprints of individual neurons (see below) in an automatic fashion.

2 Material and Methods

2.1 Cell culture preparation

Neocortical cells from newborn rats were cultured on high-density MEAs and maintained in MEM supplemented with heat-activated horse serum (5%), L-glutamine (0.5mM), and glucose (20mM) at 37 ° C and 5% CO2. The medium was partially replaced twice a week.

2.2 Material and recordings

High-density MEAs featuring 11'016 electrodes with a pitch of 18 µm were used, which permit the recording of single unit action potentials from several electrodes simultaneously. A subset of 126 channels are recordable simultaneously, and if necessary, can be re-routed to include other locations on the array.

We developed a flexible interface in C++ and Python. In order to deal with the sheer amount of data during acquisition where only meaningful signals were retained. Moreover, we performed spike-sorting to take advantage of the high spatial resolution. In order to do so, we extended to several channels a method called template-matching [2], which calculates the distance of the recorded signal to a template. Furthermore, it is known that the amplitude of the action potentials varies during a burst. Therefore, an option was implemented in the spike-sorter to rescale the signal before comparison with the template.

2.3 Footprints

Spike triggered averaging over the spiking times at the soma was computed, and footprints of such neurons representing the flux of ions through the membrane near the electrodes location show clear changes in shape and delay from one electrode to another.
In order to compute such footprints and to reduce the recording time, an algorithm was developed to automatically route the electrodes in order to track the spatial extent of individual neurons.

2.4 Network bursts

Mature culture networks of neocortical neurons exhibit periods of high synchronous activity called network bursts (NB) [3]. The propagation of activity throughout the network during such NBs follows various reproducible patterns [4], which presumably provide different synaptic inputs to individual neurons. It is of

interest, therefore, to know whether such different patterns of activity have distinguishable effects on the spatial properties of EFPs of individual neurons embedded in the network, especially at the dendritic trees.

Therefore, an on-line classification algorithm based on the recruitment order within a burst was developed and tested.

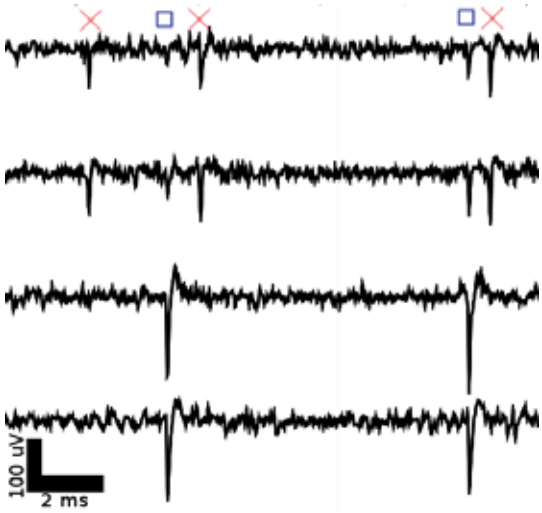

Fig. 1. Example of traces where action potentials were recordable by several electrodes simultaneously. Moreover, spikes from two neurons (red crosses and blue squares) are distinguishable. Applying a simple threshold detection on individual channels would have led to a misinterpretation of the data. For example, if one applies a threshold detection on the second channel from the top, these five spikes would have been attributed to the same neuron.

3 Preliminary results

3.1 Software interface

The software developed allows us to save the data only when activity is detected and reduces considerably the amount of data to be stored. Moreover, spike trains and ISI distribution can be displayed on-line and saved for further analysis.

3.2 Spike-sorting

The discrimination power of the template-matching algorithm applied to several channels improved greatly the quality of the spike-sorting. Qualitative analysis show that this method reduces considerably the number of false positives detected. Moreover, the spike-sorter deals adequately with the change of amplitude of the action potentials during bursts.

3.3 Footprints

The algorithm implemented improves the tracking of the individual neurons, and footprints of such neurons representing the flux of ions through the membrane near the electrodes location, and show clearly changes in shape and delay from one electrode to another. Under optimal circumstances, electrical fields can be recorded at hundreds of micrometers from the soma. The evaluation of such patterns provides useful insight about the topology of the neuron and of the different transmission delays.

Moreover, several features of individual neurons can be extracted from these footprints: the soma and the dendritic tree can clearly be differentiated due to the inversion of polarity, and smaller external electrical fields, such as the one emited by single axons, are possibly detectable. In addition to the spatial structure of individual neurons, temporal features representing the flux of ions inside the cell, as well as with the surrounding medium can also be extracted.

3.4 Classification of network bursts

The on-line algorithm succeeded in classifying the network bursts into several reliable patterns. Such feature of the program could be applied in different contexts. It is already possible to compare neuronal footprints of the same neurons embedded in different types of bursts, which is of interest since their synaptic input may vary depending on the network's activity. Moreover, such classification will be useful to apply different feedbacks to the culture while closed-loop experiments will be performed.

Acknowledgement

We thank the group of Prof. Hierlemann for providing the MEAs and for its extensive support, Samora Okujeni and Sebastian Reinarz for the cell culture preparation, and Patrick Pauli for the technical assistance. Funded by the German BMBF (FKZ 01GQ0420 & FKZ 01GQ0830) and by the EC (NEURO, No. 12788).

References

[1] Frey U, Egert U, Heer F, Hafizovic S, Hierlemann A. (2009): Microelectronic system for high-resolution mapping of extracellular electric fields applied to brain slices. Biosens Bioelectron. 2009 Mar 15;24(7):2191-8. Epub 2008 Dec 7.

[2] Rutishauser U, Schuman EM, Mamelak AN. (2006): Online detection and sorting of extracellularly recorded action potentials in human medial temporal lobe recordings, in vivo. J Neurosci Methods. 2006 Jun 30;154(1-2):204-24.

[3] Wagenaar DA, Pine J, Potter SM. (2006): An extremely rich repertoire of bursting patterns during the development of cortical cultures. BMC Neurosci. 2006 Feb 7;7:11.

[4] Raichman N, Ben-Jacob E. (2008): Identifying repeating motifs in the activation of synchronized bursts in cultured neural networks. J Neurosci Methods. 2008 May 15;170(1):96-110. Epub 2008 Jan 11.

Networks in dissociated culture follow native cortical development

Steffen Kandler[1,2,3*], Samora Okujeni[1,2,3], Sebastian Reinartz[3] & Ulrich Egert[1,3]

1 Bernstein Center Freiburg
2 Neurobiology and Biophysics, Inst. Biology III
3 Biomicrotechnology, Dept. Microsystems Engineering; ALU Freiburg, Germany
* Corresponding author. E-mail address: kandler@bcf.uni-freiburg.de

Synchronization of neuronal activity plays a crucial role for the formation of functional circuits in developing cortical networks. We investigated structural and functional development of cultured networks with combined patch-clamp and microelectrode array (MEA) recordings. We found that maturation processes in culture—*e.g.* the pairwise correlations of bursting activity—show comparable changes throughout development as observed in neonatal networks *in vivo.* This suggests that identical mechanisms also shape neuronal networks *in vitro.*

1 Introduction

The spontaneous synchronization of network activity during early cortical development supports the formation of basic functional circuits and neuronal assemblies. Recent studies argued that synchronized activity could serve as refinement mechanism of early neuronal maps and that a transition to asynchronous activity states coincides with the integration of sensory inputs, *e.g.* [1,2]. It suggests that the synchronization of activity has mechanistically a fundamental influence on the emerging computational properties of developing networks.

Here, we investigated the structural and functional embedding of individual neurons into synchronous network bursts (NB) within networks developing in dissociated culture. By monitoring these networks intracellularly and extracellularly with dual patch-clamp electrodes and MEA, we gained insight into the underlying network connectivity and the activity dynamics on a single-neuron and population level.

2 Methods

Neuronal tissue was obtained from frontal cortex of newborn rats following standard procedures [3,4]. Dissociated cells were seeded at densities of 1,500–5,000 neurons per mm^2 on PEI coated MEAs. Cultures were maintained in MEM supplemented with heat-inactivated horse serum (HS; 5%), L-glutamine (0.5 mM), and glucose (20 mM) in a humidified atmosphere at 37°C and 5% CO_2.

Combined dual patch-clamp and MEA recordings were performed to test for pairwise connectivity at a distance range of max. 400 µm and to record neuronal embedding into NB activity. Recordings were carried out at 35–37°C using a slow perfusion (100 µl/min[1]) with carbogenated (95% O_2, 5% CO_2) culture medium without HS supplement.

3 Results

Networks with seeding densities higher than 2,000 neurons per mm^2 converged to this density within four weeks *in vitro*, indicating that maturation processes limit the final network density (Fig. 1).

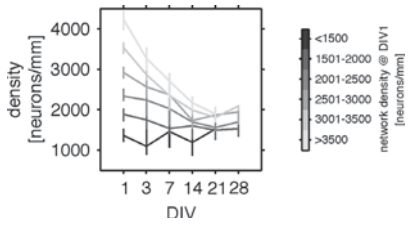

Fig. 1. Developmental decrease of network density depends on seeding density.

We observed that individual neurons were more likely to participate in NBs if those were stronger (*i.e.* higher no. of in-burst spikes or participating units) and if the NB onsets across electrodes were more synchronous (Fig. 2).

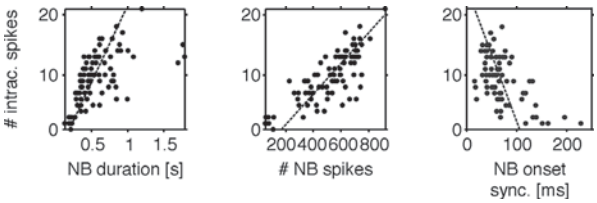

Fig. 2. Individual neuron in-burst activity correlates with NB duration (left), no. of array-wide NB spikes (center), and NB onset synchrony (right), *i.e.* the duration it takes for 25–75% of all neurons to fire their first NB spikes.

The distance dependent pairwise correlations in the firing within spontaneous NBs increased during network maturation, similar as found in native cortex [1] (Fig. 3).

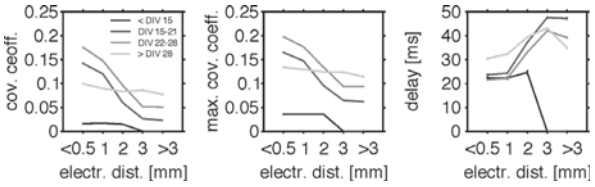

Fig. 3. Age and distance dependent increase of covariance coefficients (CC) from DIV 14–21 and equalization of CCs after DIV 21 for zero-lag CC (left) and max. CC (center). Further, max. CCs have greater delays with increased pairwise distances (right).

The onset of NBs was further restricted to distinct sets of network sites, suggesting that the spatial arrangement and connectivity of neurons in these populations support NB initiation and propagation. Pairwise correlations between intracellular and extracellular NB firing were highly dependent on NB onset latencies, and to little or no degree on the spatial distances to NB onset sites (Fig. 4).

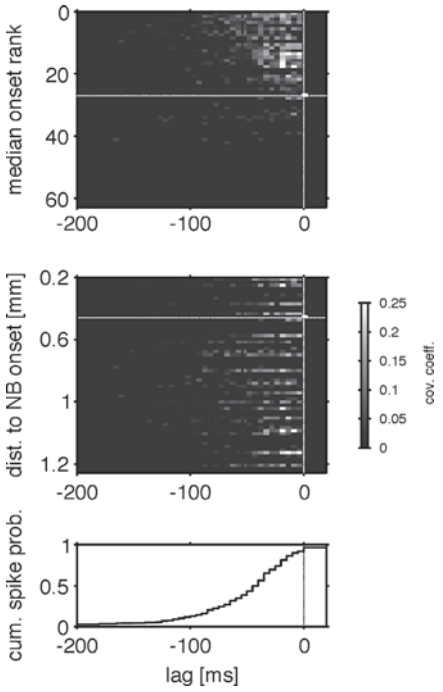

Fig. 4. Sorted pairwise correlations of intra- and extracellular NB spiking are dependent on median NB onset ranks (top) and not distance to NB onset location (center). Cumulative NB spike probability (bottom). Dashed lines indicate zero-lag (vert.) and position of intracellular recording site (horz.).

In 95 pairwise intracellular recordings we found that neurons less than 400 µm apart made connections with a high probability of 49% (Fig. 5) as observed previously [5]. Most connections thereby were unidirectional (23%) or bidirectional (20%) excitatory; only about 6% of all pairs had inhibitory connections. Furthermore, the connection probability was independent of pairwise distance and of the network density at the sampled distances.

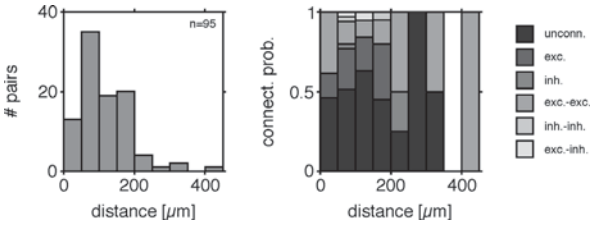

Fig. 5. Distance distribution of intracellularly recorded pairs (left) and their pairwise connection probability (right).

We also observed that EPSP amplitudes were dependent on the pairwise neuron distance and the age of the network. Herein, a separation was found for amplitude distributions of distances shorter resp. larger than 150 µm as well as a systematic shift of higher towards lower amplitudes with increased network age.

4 Discussion

Developmental changes of network synchrony in neuronal cultures show parallels to early cortical development *in vivo*. Especially, the network age dependent changes of pairwise correlations are similar to observations made in native cortex suggesting that cultured networks in principle follow the same mechanisms that refine early network structure and activity in a native context [1]. This is also supported by the developmental decrease of EPSP amplitudes which are subjected to the formation of more and more new synapses and synaptic scaling [6]. We, however, did not observe a transition of NB activity to asynchronous activity as observed *in vivo*. This could be explained by the lack of adequate input and lack of *functional* processing within the cultured networks.

Our results further suggest that a high degree of excitation and interconnectivity supports the spontaneous formation of NBs at distinct locations within the networks. The comparatively low number of inhibitory connections could partly result from maturation processes differentially advanced in excitatory and inhibitory subpopulations at the time of tissue preparation and during culture development [7].

Acknowledgement

Clemens Boucsein is warmly thanked for his support on intracellular recording techniques. Patrick Pauli and Ute Riede are thanked for technical assistance.

This work was supported by the German BMBF (BCCN, FKZ 01GQ0420 & BFNT, FKZ 01GQ0830) and by the EU (NEURO, No. 12788).

References

[1] Golshani *et al.* (2009) *J Neurosci 29(35):10890–10899.*
[2] Luczak *et al.* (2007) *PNAS 104(1):347–352.*
[3] Shahaf & Marom (2001) *J Neurosci 21(22):8782–8788.*
[4] Potter & *DeMarse.* (2001) *J Neurosci Meth 110:17–24.*
[5] Nakanishi & Kukita (1998) *Brain Res 795:137–146.*
[6] Garner *et al.* (2006) *Cell Tissue Res 326:249–262.*
[7] De Lima & Voigt (1999) *Eur J Neurosci 11:3845–3856.*

How to Reduce Stimulus/Response Variability in Cortical Neuronal Networks

Oliver Weihberger[1,2,3*], Samora Okujeni[1,2,3] , Ulrich Egert[1,3]

1 Bernstein Center for Computational Neuroscience Freiburg
2 Faculty of Biology
3 IMTEK - Department of Microsystems Engineering
University of Freiburg, Freiburg, Germany
* Corresponding author. E-mail address: weihberger@bccn.uni-freiburg.de

Repeated application of the same electrical or sensory stimulus evokes varying responses in neuronal networks. Independent of top-down influences such as behavior, attention or conscious state, this can be attributed to interactions between ongoing and evoked activity. The state of the network at the moment of stimulation critically determines over the evoked response. The goal of this study was to identify low-level mechanisms that underlie the modulation of stimulus/response relations. We aimed for predictive models and reproducible responses in targeted interaction with neuronal network activity.

1 Introduction

One of the most astonishing features of the central nervous system is its functional power in spite of its variability – the same stimulus elicits different responses in repeated trials. Our behavior, attention or conscious state alters the way external stimuli are processed and information is represented. While learning represents a directed, long-term modification of stimulus/response relations, undirected changes on shorter time scales were ascribed to interactions between ongoing and evoked activity.

Various means were used to describe this interrelation. In general, low levels of pre-stimulus activity led to stronger responses and shorter delays [1-3]. The identification of precise functional relations and the coupling to ongoing spiking activity deserves a closer study.

Understanding the mechanisms of stimulus/response modulation becomes increasingly important for neurotechnological applications. A reliable operation of e.g. visual or auditory cortical implants requires to feed defined patterns of activity into the dynamics of ongoing activity.

We recorded and stimulated cortical cell cultures on microelectrode arrays (MEAs). Electrical stimuli were placed randomly in between periods of synchronous network-wide bursting. User-defined interaction with network activity controlled the stimulus timing relative to ongoing bursting activity. Stimuli were placed at pre-defined states of network inactivity. This enhanced response reproducibility and facilitated the examination of state-dependent input/output relations.

2 Material and Methods

2.1 Cell culture preparation

Cells from prefrontal cortical tissue of neonatal wistar rats were cultured on polyethylene imine-coated MEAs. Cultures were maintained in MEM supplemented with heat-inactivated horse serum (5%), L-glutamine (0.5 mM), and glucose (20 mM) at 37º C and 5% CO_2. Medium was partially replaced twice per week.

2.2 Recording and stimulation

A Multi Channel Systems MEA1060BC amplifier, STG2008 stimulus generator and MeaBench [4] were used for recording and stimulation inside the incubator. Monophasic negative voltage pulses, width 400 µs, amplitudes ≥ 0.4 Volt were used. Stimuli were triggered either *i)* at fixed inter-stimulus intervals (IstimI) of 10 or 20 sec., or *ii)* after a defined period without spike (post-burst interval) from a selected feedback site has passed. A minimum IstimI of 10 sec. was enforced.

3 Results

3.1 Response delays decreased with longer duration of pre-stimulus inactivity

The duration of pre-stimulus inactivity modulated response delays. Long periods of inactivity led to small delays. Bursting activity prior to stimulation led to large delays. Millisecond response delays were determined by the pre-stimulus activity on a time scale of seconds (Fig. 1).

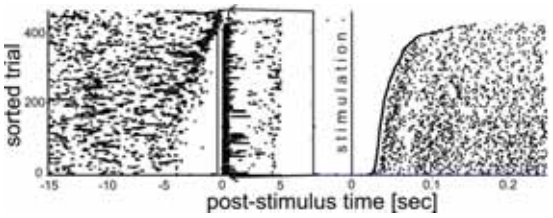

Fig. 1. left: raster plot, recording site 22. 471 stimuli with 20 sec. IsimI applied at site 67. Trials were sorted for increasing response delay. right: zoom in around stimulation. Note the increasing delays from ≈ 25ms to ≈ 125 ms and the corresponding arrangement of pre-stimulus activity.

3.2 Control of stimulus timing enhanced response reproducibility

Post-burst stimulation controlled the timing of stimulation relative to ongoing activity. Responses became more regular. Response variability (standard deviation (std) of response length normalized by the std of spontaneous burst length) decreased. Single-site reliability (no. responses / no. trials) increased compared to fixed-interval stimulation (Fig. 2).

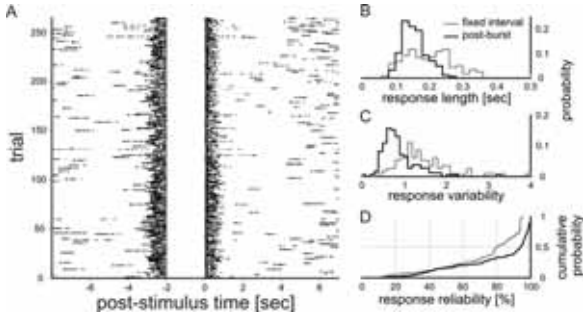

Fig. 2. Post-burst stimulation **A**, raster plot, recording site 14. Pre-stimulus bursts terminated at the same time. The state of the network was comparable in each trial. **B-D,** Statistical comparison to fixed-interval stimulation. Responses were shorter and more narrowly distributed (B), Response variability decreased (C), reliability increased (D). 119 (fixed-interval) resp. 185 recording sites with 1, 1.5 or 2 sec. post-burst interval were analyzed.

3.3 Network-state dependent propagation speed

Post-burst stimulation facilitated a controlled examination of state-dependent stimulus/response relations. Response delays increased with distance to stimulation site. That is, the initial focus of activation propagated from the site of stimulation. Propagation paths were independent of the network state. Propagation speed, however, was faster for longer pre-stimulus inactivity (Fig. 3).

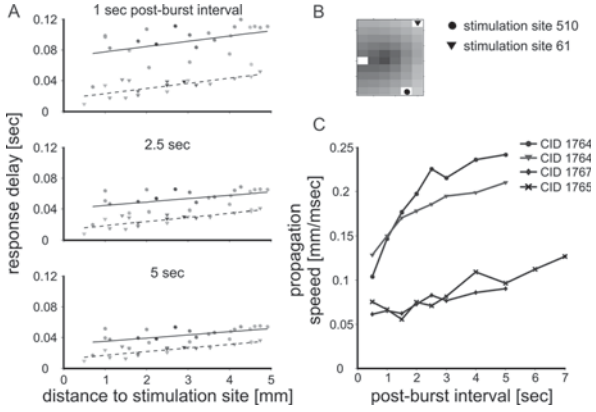

Fig. 3. A, B, Stimulation with 8 different post-burst intervals at two different sites. Approx. 250 trials in each case (B). Response delays increased with the distance to stimulation site. The direction of propagation was maintained (A). **C**, Propagation speeds increased with longer duration of pre-stimulus inactivity. 4 recordings analyzed.

4 Conclusion

Synchronous network-wide bursting modulated stimulus/response relations. The duration of pre-stimulus inactivity critically determined response properties. We propose that activity-dependent synaptic depression shuts down excitability. Subsequent recovery entails shorter delays. Targeted interaction with ongoing activity confined response variability.

Acknowledgement

We thank S. Kandler for valuable help in cell culturing and Patrick Pauli for technical assistance. This work was supported by the German BMBF (FKZ 01GQ0420 & FKZ 01GQ0830) and by the EC (NEURO, No. 12788).

References

[1] Arieli A., Sterkin A., Grinvald A., Aertsen A. (1996). Dynamics of ongoing activity: explanation of the large variability in evoked cortical responses. *Science*, 273, 1868-1871

[2] Kisley M.A., Gerstein G.L. (1999). Trial-to-trial variability and state-dependent modulation of auditory-evoked responses in cortex. *J. Neurosci*., 19, 10451-10460

[3] Azouz R., Gray C.M., (1999). Cellular mechanisms contributing to response variability of cortical neurons in vivo. *J. Neurosci.*, 19, 2209-2223

[4] Wagenaar D., DeMarse T.B., Potter S.M. (2005). MeaBench: A toolset for multi-electrode data acquisition and on-line analysis. *Proceedings of the 2nd International IEEE EMBS Conference on Neural Engineering, 16-19 March 2005*, 518-521.

Calcium dynamics during bursting activity in neocortical cultures

Matthew Goddard[1*], Ulrich Egert[1,2]

1 Bernstein Center Freiburg, Univ. of Freiburg, Germany
2 IMTEK - Department of Microsystems Engineering, Univ. of Freiburg, Germany
* Corresponding author. E-mail address: matthew.goddard@bcf.uni-freiburg.de

Calcium influx during periods of bursting activity in primary dissociated cortical cultures was investigated. We used a marker for live cell calcium imaging combined with MEA recordings in 21-53 DIV cultures and found that multi-electrode site bursting, rather than single spikes, were associated with calcium transients during spontaneous network activity. Furthermore, spatio-temporal cell firing patterns tended to be conserved during bursts, despite subtle differences in burst propagation patterns.

1 Introduction

1.1 Calcium and signalling

Calcium (Ca^{2+}) imaging of neural cells provides a useful measure of cell excitability, for example in the detection of action potentials [1, 2, 3], as well offering the capability for sampling at a high spatial resolution (e.g., up to 610 mm² at 10x magnification, [4]). Recently it was shown that Ca^{2+}transients in cultured networks are reliably coupled to bursts, and that strength of this coupling is modified by the age of the culture [5]. However, it is also known that network firing activity and burst properties, such as burst duration and electrode participation, depend on a number of factors including seeding density [6]. In the present study one of the aims was to characterise in greater detail the relationship between peri-burst calcium transients in young (2-3 wks) and old (>7 wks) cultures with comparable seeding densities. We also sought to explore the dynamics of individual cell recruitment during bursts and how this may be modified by factors such as distance to burst onset, burst propagation, and electrode site recruitment (i.e., size of network burst). Glial cell calcium transients were of particular interest because of the capacity of glia to modulate neuronal activity [7]. Thus, as a final objective, we characterised peri-burst calcium transients in astrocytes as well as neurons [4, 8].

2 Methods

2.1 Cultures

Neocortical tissue was harvested from Wistar rat pups at PN0. Cortical cells were dissociated and cultured on 6x10 (500/30) or 8x8 (200/30) MEAs at an initial density of approx. 6000 cells/mm2 for up to 53 days in vitro (DIV).

2.2 Calcium imaging

Cultures were bulk-loaded with 9 μM Fluo4AM (Molecular Probes F14201) at 25˚C for 25 min. Fluorescence imaging (Zeiss Examiner Z1) was performed using an excitation light source of 470 nm (Colibri, Zeiss) for 2-4 min per recording frame area (692x520 pixels). Emitted light (~515 nm) was filtered (AHF, F66-422) and recorded via CCD camera to a PC at 12.5 Hz (Axiovision software). Imaging data was preprocessed by manual region-of-interest (ROI) pixel mapping and analysed with MEA activity in Matlab R2009b and OOCalc. Cells were classified functionally as neurons or as astrocytes according to their calcium transient onset kinetics and durations [4, 8].

2.3 MEA recordings

Electrical recordings were sampled at 25 KHz using Multichannel Systems software (MCRack, v3.8). Spike cutouts were generated by thresholding baseline activity at -5 stdev. Bursts were detected offline in MCRack using the following interspike-interval (ISI) parameters: Max ISI to start burst, 60 msec; Max ISI to end burst, 120 msec; Min inter-burst interval, 300 msec; Min burst duration, 50 msec; Min no. spikes per burst, n = 5. Network bursts were defined in OOCalc as having: multi-site burst onsets occuring within 50 msec; and a minimum 3 site recruitment.

3 Results

3.1 Ca^{2+} transients

28% (mean; +/- s.d. 18%) of the visible cells of a 22 DIV culture showed measurable changes in

calcium fluorescence, vs. 17% (mean; +/- 2% s.d.) for a 56 DIV culture. Two types of transient profiles were observed: fast onset (0.22 sec, mean; +/-0.15, s.d.) with relatively short duration (2.49 sec, mean; 1.18, +/- s.d.), i.e., consistent with neurons; and slower onsets (1.5 sec, mean; +/- 1.89, s.d.) with longer durations (7.83 sec, mean; +/- 5.64, s.d.), i.e., consistent with astrocytes.

3.2 Ca^{2+} transients during bursts

Bursts in the 56 DIV culture occurred at a rate of 13.33 bursts/min with a mean 40 electrode recruitment, vs. 2.32 bursts/min across 30 electrodes in the 22 DIV culture. Neuronal Ca^{2+} transients, irrespective culture age, were coupled to bursts with 97.7% coherence and by an average delay of 2.5 msec (+/- 98 msec s.d.). Glial Ca^{2+} transients were often associated with bursts (76% coherence), but with greater variability in their relative onset times (-414.5 msec, mean; +/- 1.06 sec, s.d.). Burst duration did not predict neuronal Ca^{2+} transient duration (RSq.<0.1), and was only a weak predictor for glial transient duration (RSq.=0.15).

3.3 Propagation patterns

Network burst propagation patterns consisted of several different motifs during each 2-4 min recording period (e.g., Fig. 1). Individual cell recruitment into network bursts was analysed using a Sørensen similarity index, yielding values ranging from 0.4 to 0.95. Duration of network burst, distance from burst origin to cells within the recording frame, and number of participating electrodes were not reliable predictors for the degree of similarity of individual cell recruitment (respectively, RSq. <0.1; RSq.=0.14; RSq.<0.1).

4 Discussion

Calcium transients were observed to be coupled to bursts in both neurons and glial cells, in both 22 and 56 DIV cultures. Whereas neuronal calcium transients showed well-defined onsets, coinciding with bursts, glial cell transient onsets were highly variable with respect to burst onsets. Slow Ca^{2+} transient kinetics in these cells made it difficult to identify precise onset times, however. It is not yet clear under which conditions the greatest degree of coupling occurs between glial and neuronal Ca^{2+} transients during bursts. However, there was an indication in neuronal cells at least that the number of participating electrodes depended on a common pool of 'initiator' sites within the culture recruiting other parts of the network; and provided that a minimum of three electrode sites were recruited then the level of similarity in individual cell recruitment was relatively conserved.

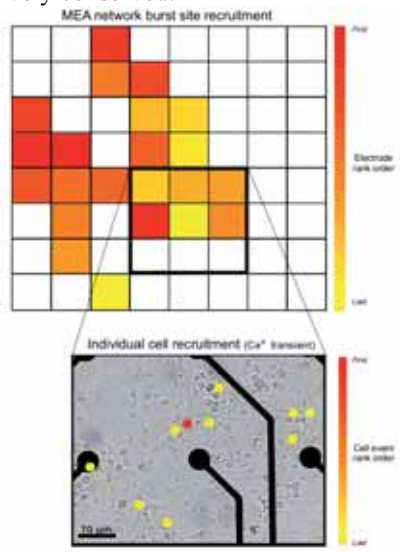

Fig. 1. A spontaneous propagation motif. Top: Schematic layout of MEA showing network burst propagation pathway by site recruitment order. Bottom: Optical recording frame (200x magnification) showing individual cell recruitment by calcium transient onset order within the optical recording frame.

Acknowledgements

We thank Uni-Freiburg, the BCF, and IMTEK for the resources to carry out this research, as well U. Reide and P. Pauli for their assistance and culture preparations. Funding was provided by the German BMBF (BCCN Freiburg FKZ 01GQ0420 Freiburg*Tübingen FKZ 01GQ0830).

References

[1] Opitz, T., Lima, A, D, D., Voigt, T. (2002): Spontaneous development of synchronous oscillatory activity during maturation of cortical networks in vitro. *Journal of Neurophysiology, 88, 2196-2206*

[2] Smetters D., Majewskat A., Yuste, R. (1999). Detecting action potentials in neuronal populations with calcium imaging. *Methods: A Companion to Methods in Enzymology*, 18, 215-221.

[3] Regehr, W. G., Atluri, P. P. (1995): Calcium transients in cerebellar granule cell presynaptic terminals. *Biophysical Journal, 68(5), 2156-2170*

[4] Ikegaya, Y., Bon-Jego, M. L., Yuste, R. (2005): Large-scale imaging of cortical network activity with calcium indicators. *Neuroscience Research, 52, 132-138*

[5] Takayama, Y., Moriguchi, H., Kotani, K., Jimbo, Y. (2009): Spontaneous calcium transients in cultured cortical networks during development. *IEEE Transactions on Biomedical Engineering, 56(12), 2949-2956*

[6] Wagenaar, D. A., Pine, J., Potter, S. M. (2006): An extremely rich repertoire of bursting patterns during the development of cortical cultures. *BMC Neuroscience, 7(11), 1-18*

[7] Haydon, P. G. (2001): Glia: Listening and talking to the synapse. *Nature Reviews Neuroscience, 2, 185-193*

[8] Takahashi, N., *et al*., (2007): Watching neuronal circuit dynamics through functional multineuron calcium imaging (fMCI). *Neuroscience Research, 58, 219-225*

Electrical Stimulation, Implants and Robotics

Electric Stimulation Of Explanted Retina Using A Subretinal Implant Chip In A Video Projector Setup

Andreas Padberg[1, 2*], Steffen Kibbel[3], Thoralf Herrmann[1], Ulrich Egert[2], Alfred Stett[1]

1 NMI Natural and Medical Sciences Institute at the University of Tuebingen, Reutlingen, (Germany)
2 IMTEK, Biomicrotechnology, Albert-Ludwigs-Universität Freiburg, Freiburg, (Germany)
3 Retina Implant AG, Reutlingen, (Germany)
* Corresponding author. E-mail address: Andreas.Padberg@NMI.de

A light-sensitive stimulation chip from a subretinal implant system was used for electric stimulation of degenerated retinal tissue. The constructed setup mimics the clinical implant situation. Ganglion cell response upon stimulation was recorded. Results indicate functional lateral interactions within the degenerated retina.

1 Introduction

Retinitis pigmentosa (RP) leads to gradual degeneration of photoreceptor cells in human retina, ultimately causing blindness. Despite loss of photoreceptor- and horizontal cells, remaining bipolar and ganglion cell populations show little decay. The subretinal implant (Retina Implant AG) contains a light sensitive photodiode-array with corresponding stimulation electrodes. Subretinal implanted between pigment epithelia and neural retina, the implant resumes the function of photoreceptor cells by electrical stimulation of bipolar cells [1, 2]. Electric stimulation of bipolar cells causes correlated activity in ganglion cells, and evokes perception of phosphenes in humans with advanced RP. Patients with a subretinal implanted chip perceived phosphenes in an orderly fashion, reflecting shapes and sizes of objects in their environment, one patient even regained the ability of reading large letters [3].

We developed a setup for conducting electrophysiological research on underlying biological mechanisms (Fig.1). The retinal implant chips were used for continuous electrical stimulation of degenerated retinal tissue from an RP-model (RCS-Rat) with a fixed frequency of 5 Hz and pulse duration of 500µs.

2 Materials and Methods

Visual pattern are generated, using a PC and the psychologist toolbox for Matlab [4, 5]. Patterns are presented via a LCD-projector focused and coupled through a binocular. Focal planes of binocular and video projector are adjusted to match the chip's surface. The chip contains 40 x 40 pixels with a pitch of 70 µm covering an area of 3 x 3 mm. Each pixel contains a micro-photodiode to detect light-intensity, a circuit to convert the detector signal into a stimulating voltage and a 50x50 µm² TiN stimulation electrode. The sensitivity and gain of the chip can be adjusted. The chip is mounted on a carrier providing electric connection, allowing application, perfusion and temperating of retinal tissue. Adjustment of the chip to illumination levels of patterns, frequency and pulse duration are set with the chip's stimulus generator.

Samples from explanted retinas are placed ganglion cell up on the chip surface (Fig. 2). For proper handling, the retina was mounted on a nitrocellulose filter with a punched opening with 2 mm diameter. Extracellular recording of ganglion cell activity is conducted with a needle electrode, mounted to a micromanipulator and lowered onto the ganglion cell layer under visual control. Signals are amplified and recorded, together with timestamps of chip's stimulation pulses, and timing of light stimulus on- and offset. Spike activity is extracted and correlated to the stimulus using Matlab.

3 Results

Ganglion cell activity from retina samples placed on a chip could be recorded for up to 7 hours. Visual patterns are converted to electric stimulation patterns via the chip. Cell activity can be modulated with different levels of brightness. Activity was correlated to temporal and spatial change of illumination only when the chip was activated (Fig. 3). Ganglion cells increased or decreased spiking activity upon electric stimulation. Response to both on- and offset of stimulus and on-/off- receptive field structures were observed (Fig. 4).

4 Discussion

Functionality of the setup for electric stimulation of degenerated retinal tissue with visual patterns was shown. Different types of response were recorded. Results indicate functional lateral interactions within the degenerated retina. The setup is advantageous for experiments with moving patterns. However, chip electrode spacing and binocular magnification limits spatial resolution. Further experiments will investigate functionality of remaining lateral amacrine network,

and pathways of synaptic transmission upon electric stimulation, with a pharmacological approach.

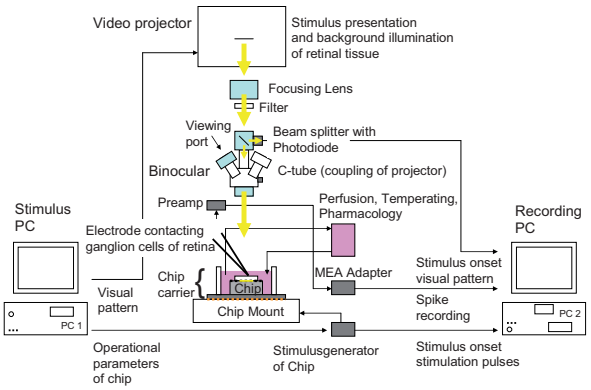

Fig. 1. Main components of the setup for stimulation of retinal samples attached to light-sensitive stimulation chip.

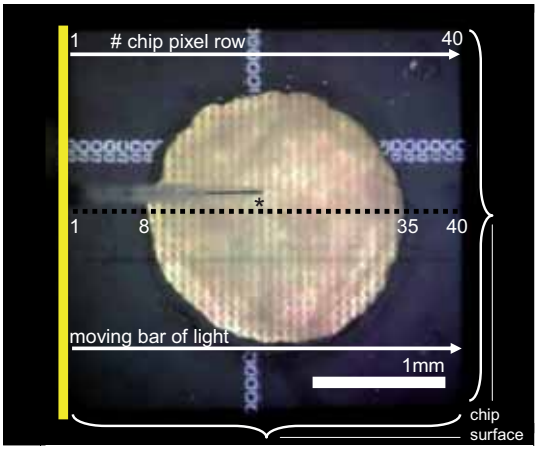

Fig. 2. Top view on chip with attached retina (see text). For experiments in Fig.4., a light bar presented on dark background moved with constant motion from left to right across all 40 chip pixel rows. * Position of needle electrode for spike recording.

Acknowledgement

This work was supported by the German Ministry for Education and Research (BMBF), grant 0315113 to Retina Implant AG.

References

[1] Stett A., Mai A., Herrmann T. (2007). Retinal charge sensitivity and spatial discrimination obtainable by subretinal implants: key lessons learned from isolated chicken retina. Journal of Neural Engineering 4, S7-S16

[2] Gerhardt M, Alderman J, Stett A. (2010). Electric field stimulation of bipolar cells in a degenerated retina - a theoretical study. IEEE Trans Neural Syst Rehabil Eng. 18(1):1-10.

[3] Zrenner E, et al. (2009) Subretinal Microelectrode Arrays Allow Blind Retinitis Pigmentosa Patients to Recognize Letters and Combine them to Words. Biomedical Engineering and Informatics 2, 1-4.

[4] Brainard, D. H. (1997) The Psychophysics Toolbox, Spatial Vision 10: 433-436.

[5] Pelli, D. G. (1997) The VideoToolbox software for visual psychophysics: Transforming numbers into movies, Spatial Vision 10: 437-442.

.

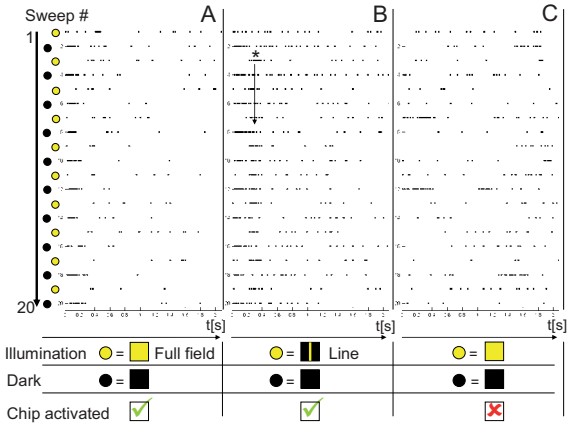

Fig. 3. Rasterplot of a ganglion cell's activity (on-/off type). Two seconds of spike events are shown in each line. Light condition switched from dark to bright illumination every 5 seconds with 20 repetitions. **A**) Full field illumination: Transient increase of activity to stimulus offset. **B**) Stationary line illumination (70 µm bar of light at central position of chip): Additional, short and delayed increase of activity to stimulus onset. *Differences between A and B indicate retinal network activity. Additional response to stimulus onset in B might appear due to lacking inhibition from lateral areas, with less retinal surface being stimulated than in A. **C**) Control with deactivated chip.

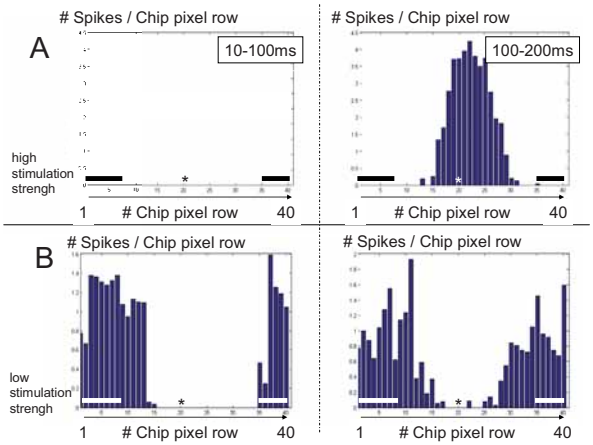

Fig. 4. Stimulation-strength-dependent on-/off-response of a ganglion cell. A light bar moved from left to right across a retina attached on the chip (see Fig.2.). Bar velocity 250 µm/s, bar diameter 70 µm. Spike rates are calculated for the time windows 10-100 ms and 100-200 ms after the electric stimulation pulses. Spike rates are plotted against the position of the light bar on the chip, and averaged for 15 repetitions of bar movement across the chips surface. The histogram column for a chip pixel row shows the number of average spike events that occurred within the timeframe the light bar took to move across that row. Thus a map of the activity induced from each of the 40 chip electrode rows is generated, and displays the cells receptive field upon electric stimulation in direction of the x axis. **A**) High stimulation strength / On-component: Spontaneous activity is actively suppressed by charge that is delivered by chip under dark condition (dark background illumination). Increase of charge transfer as light bar enters area of exposed photodiodes elicits central on-response. **B**) Low stimulation strength / Off-component: Spontaneous activity is actively suppressed when the light bar enters receptive field area, but charge is insufficient to elicit on-response. Gap between black bars (A) and white bars (B) indicates area of exposed photodiodes. * Position of recording electrode.